Electrostatic Stabilization in Myoglobin. Interactive Free Energies between Individual Sites†

Stephen H. Friend and Frank R. N. Gurd*

ABSTRACT: The pattern of electrostatic interactions between pairs of charge sites in sperm whale ferrimyoglobin was examined as a function of pH in terms of proton site occupancy, static solvent accessibility, and distance of separation. By grouping all examples of the most stabilizing interactions and all examples of the most destabilizing interactions, we can easily show that at pH 7.50 the former is much stronger; that is, the negative contributions to electrostatic free energy far outweigh the positive contributions. Much of the electrostatic energy of stabilization in native myoglobin is provided by specific charge-pair partners that are very highly conserved among 53 mammalian myoglobin species and is invariant substantially from pH 8.5 to 3.5. Destabilizing interactions that become most significant, but not actually dominant, near the acid unfolding pH range can be recognized in emerging clusters of uncompensated positive charges. Binding of azide ion by the heme iron effectively reduces the most prominent destabilizing set of such interactions. In general, those charged residues that experience the largest summed stabilizing interactions with other groups are the most conserved between species. The histidine residues, however, show their best correlation of conservation with low values of static accessibility. Although histidine residue 64 has an effective pK corresponding to the midpoint of the unfolding transition near pH 4.2 at an ionic strength of 0.10 M and so might be called a "trigger group", its interactions contribute only a modest fraction of the overall pH-dependent free energy change. An examination of the primary stabilizing interactions represented by the charge-pair partners indicates a probably major role of electrostatic interactions in the nucleation and docking stages of the condensation of the polypeptide chain into the compact native structure.

The preceding paper in this issue (Friend & Gurd, 1979) extended the consideration of electrostatic effects in sperm whale ferrimyoglobin (Shire et al., 1974a,b, 1975; Botelho et al., 1978) to the analysis of the pH-dependent unfolding in acid solution and of the overall electrostatic contribution to the stability of the molecule. The importance of ionic interactions for stability was demonstrated experimentally by the marked dependence of the unfolding process on ionic strength. Knowledge of the specific pK values for individual titrating sites through use of the modified Tanford–Kirkwood theory (Tanford & Kirkwood, 1957; Tanford & Roxby, 1972; Shire et al., 1974a) provided the basis for analyzing summed electrostatic interactions. The computed pH dependence of the summed net electrostatic stabilization was shown to correspond (Friend & Gurd, 1979) with the pH dependence of the thermal stability of the sperm whale ferrimyoglobin (Acampora & Hermans, 1967). These results add to the previously established success of the modified treatment in predicting pK values in myoglobins (Shire et al., 1974b, 1975; Botelho et al., 1978). The application of the treatment to other small, globular proteins has been reported (Matthew et al., 1978b, 1979a,b).

Several questions pertaining to interactions between charged sites have been raised in the past (Linderstrøm-Lang, 1924; Tanford, 1961; Clark & Gurd, 1967; Gurd & Rothgeb, 1979), which can be cautiously addressed in the light of the theoretical computations of interaction energies between individual charged sites. The following are some of these questions. (1) How significantly different are the stabilizing or destabilizing interactions involving a given charged group when neighboring groups titrate as the pH is varied? (2) What proportion of the total electrostatic interaction energy between pairs of charged sites represents destabilizing interactions under conditions of strong overall net stabilization? (3) Considering amino acids as chemical classes, how varied are the interactions in given classes at various pH values? (4) Considering substitutions of residues among different animal species, are the individual charge-bearing residues that are involved in the most highly stabilizing interactions preferentially conserved relative to those that play less marked roles in electrostatic stabilization? (5) Is it possible to define specific regions of the molecule in which electrostatic interactions are critical for the unfolding process in acid solution? These questions will be considered in the present instance in terms of intramolecular electrostatic interactions in the neutral and acid pH range for sperm whale myoglobin.

Experimental Section

Stability Measurements. Ferrimyoglobin was prepared and stability measurements were made as described in the preceding paper in this issue (Friend & Gurd, 1979). Azide myoglobin was prepared from aquoferrimyoglobin by incorporation of 0.20 mM NaN_3. Denaturation measurements were made at the azide ferrimyoglobin Soret band at 422 nm where the molar extinction coefficient is 110000 cm/M (Nakhleh, 1971).

Computation and Computer Graphics. The computational procedures have been described in the preceding paper in this issue (Friend & Gurd, 1979). Three-dimensional bar graphs were generated by using a Fortran program written for that purpose and run on a CDC 6600 computer interfaced with a Versatek 1200 plotter. Potential energy surfaces were generated on similar equipment by using a program kindly provided by Professor J. Hepner of the I. U. Computing Center, Bloomington, IN.

Results and Discussion

Magnitude of Individual Electrostatic Interactions. The most elementary level on which to consider electrostatic interactions is between pairs of individual charge sites. These interactions are conveniently discussed first to define the limits

† From the Department of Chemistry and the Medical Sciences Program, Indiana University, Bloomington, Indiana 47405. *Received April 13, 1979.* This work was supported by U.S. Public Health Service Research Grant HL-05556. This is the 110th paper in a series dealing with coordination complexes and catalytic properties of proteins and related substances. For the preceding paper see Friend & Gurd (1979).

0006-2960/79/0418-4620$01.00/0

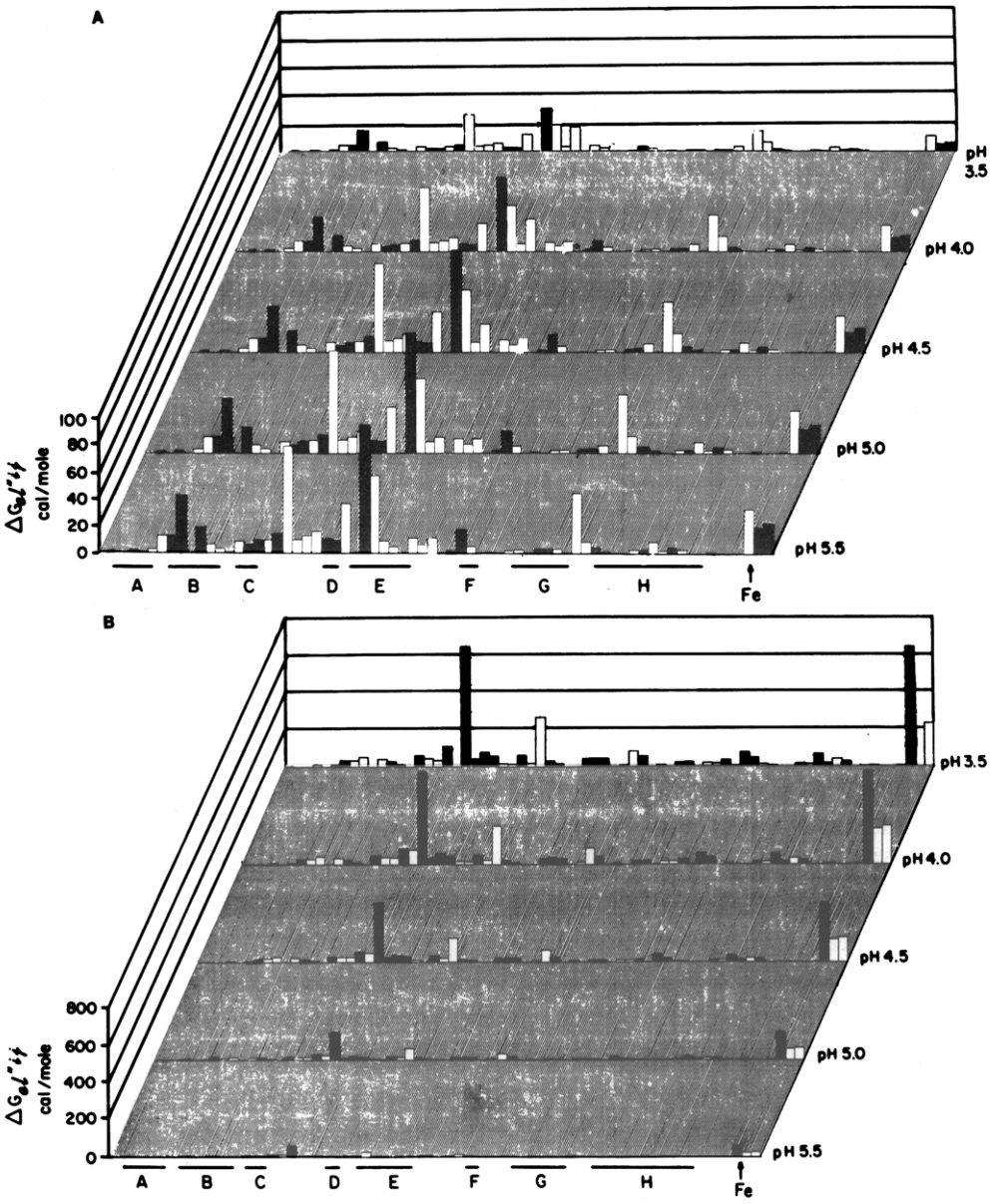

FIGURE 1: (A) Computed free energy of electrostatic interaction, $\Delta G_{el}''$, in calories per mole, between each charge site and Glu-59. The diverse charge sites are indicated in terms of their helix references; the iron site is marked at the right-hand end and is followed by the propionic acid sites. Negative (stabilizing) free energies are denoted by open bars, and positive (destabilizing) free energies are denoted by solid bars. The results are shown for the pH values 5.5, 5.0, 4.5, 4.0, and 3.5 for an ionic strength of 0.01 M and 25 °C. (B) The corresponding interactions between each charge site and His-64.

that frame other considerations of the effects of given residues and collections of residues in the protein.

As shown in the preceding paper in this issue (Friend & Gurd, 1979), the electrostatic free energy of interaction of two charged sites, i and j, can be represented by

$$W_{ij}'' = W_{ij}(1 - SA_j)(1 - SA_i) \quad (1)$$

where W_{ij} is the electrostatic work term for placing the charges on the equivalent sphere under conditions of equilibrium occupancy of all other sites and SA_j and SA_i are the static accessibility values for the respective sites. These individual W_{ij}'' terms, multiplied by Z_iZ_j to allow for fractional occupancy of each site at fixed pH and ionic strength, express the free energy of the isolated interaction between the two charge loci, $\Delta G_{el}''$, under given conditions.

Figure 1A is a three-dimensional bar graph representing the value of $\Delta G_{el}''$ between Glu-59 and each of the other charge sites, j, numbering 58 in all. The various interacting sites are shown along the lower border with the helix segments lettered (Watson, 1969). In addition to the 153 residues of the protein moiety, providing 55 of the other charge sites, there are shown at the right-hand end the iron atom (keyed hereafter as item 154) and the two propionic acid groups (items 155 and 156). The left-hand ordinate indicates the scale of $\Delta G_{el}''$ that applies to the bar graphs expressed in units of calories per mole. The results are shown for a series of five pH values from 5.50 to 3.50. The computations are made for 25 °C and an ionic strength of 0.01 M. Stabilizing interactions of positively charged groups with Glu-59 are shown as open bars, and destabilizing interactions with negatively charged groups are shown as filled bars, denoting negative and positive values of $\Delta G_{el}''$, respectively. Note that as the pH is lowered both negative and positive values of $\Delta G_{el}''$ generally decrease in Figure 1A, the former because protonation of Glu-59 gradually diminishes Z_i and the latter because both Z_i and Z_j for negatively charged groups decrease in the pH range depicted. Note that in some cases the acquisition of a positive charge by a group with a relatively low $pK_{1/2}$ (e.g., His-119) may

increase some negative values of $\Delta G_{el}''$ in the first two or three rows.

The choice of Glu-59 for illustration in Figure 1A was made because it is a relatively isolated site with a relatively low 1 − SA of 0.30. Both factors make for small absolute values of $\Delta G_{el}''$ (Friend & Gurd, 1979). Glu-59 is over 8 Å away from any other charged group. The most obvious effect of its seclusion from other charged sites is the low absolute magnitude of all of its interactions ($\Delta G_{el}'' < \pm 100$ cal/mol). Another reason for the choice is that this glutamic acid residue has the highest $pK_{1/2}$ value among all the acidic groups, 4.01. This high $pK_{1/2}$ value results in the steady decrease of interactive energies remarked on above for nearly all $\Delta G_{el}''$ values as the pH is decreased in the range in question. More important, the $pK_{1/2}$ value of 4.01 is closest to its pK_{int} of 4.50 of any negative group, which is a way of saying that it senses the least positive environment of any acidic residue and so experiences the least negative $\Delta G_{el}''$ values, i.e., the weakest stabilizing interactions. Remarkable is the fact that, despite this distinction, the majority of the interactions between Glu-59 and the rest of the molecule are stabilizing ones. Note also the widespread nature of its interactions throughout the molecule.

Figure 1B is another three-dimensional bar graph in the same form. Here, the very different example of His-64 is shown in relation to the rest of the charge sites in the molecule. The His-64 residue (the distal histidine) has the lowest $pK_{1/2}$ of any of the positively charged groups, 4.20 (Friend & Gurd, 1979).[1] The negative values of $\Delta G_{el}''$ are again expressed by open rectangles and represent negatively charged partners of His-64, and the positive values correspondingly refer to positively charged partners. Note that His-64 and Glu-59 have $pK_{1/2}$ values within 0.2 unit of each other and fall hardly more than one turn to the E helix apart. Nevertheless, comparison with Figure 1A shows vastly different interaction patterns. In the case of His-64, the positive charge is acquired in a pH range well below the pK_{int}, i.e., in a predominantly positively charged environment, and the 1 − SA value is 0.95. The protonation site N^{π} is only 5.8 Å away from the iron atom and 5.0 Å away from Arg-45. This strong positive environment both makes protonation difficult, thereby lowering $pK_{1/2}$, and produces these two most strongly destabilizing interactions that occur in the molecule at low pH. The strength of these interactions is expressed by the difference in the vertical $\Delta G_{el}''$ scale in Figure 1B relative to that of Figure 1A. While the majority of the interactions with all other groups felt by His-64 are actually stronger than those felt by the more isolated Glu-59, His-64 is an example of a site interacting predominantly with a small number of sites.

Limits of Stabilizing and Destabilizing Interactions in Myoglobin. Since proteins are not hypothetical charge clusters but instead constitute macromolecules with specific structural and functional limits that are closely guarded from the standpoint of stability and functional efficiency, it is most informative to examine the limits that apply to the interactions between the various sites. It is the upper rather than the lower limits of the absolute values of $\Delta G_{el}''$ that place boundaries on the behavior of the protein, and these upper limits of both stabilizing and destabilizing interactions are considered next. Accordingly, the most stabilizing interaction of each charged site is recorded in terms of negative values of $\Delta G_{el}''$ against the particular distance of separation, r_{ij}, in Figure 2A, and, conversely, the most destabilizing interactions are expressed as positive values of $\Delta G_{el}''$ in Figure 2B. In each figure a solid curve is included to show the effectively maximum interactions that would occur if each partner had a 1 − SA value of 0.95. The conditions illustrated are 25 °C, pH 7.50, and an ionic strength of 0.01 M. All sites are symbolized according to specific amino acid classes to distinguish the glutamic acid, aspartic acid, histidine, lysine, and arginine side chains, the terminal residues, the iron atom, and the propionic acid moieties.

The strongest stabilizing interactions in Figure 2A represent a number of cases in which charge pairs are found at distances of separation of approximately 2–4 Å. Since these pairings represent the strongest interaction experienced by each member of the pair, the symbols are overlaid. In other cases such a mutual primacy does not hold; for example, Arg-31 interacts most strongly with Glu-109, whereas Glu-109 in turn experiences its strongest stabilizing interaction with Arg-139 that can be seen to be paired with Glu-136. Note that the majority of the upper limit stabilizing interactions shown in Figure 2A do not involve charge pairs.

One more point stands out from Figure 2A. The computed interactive energies are generally less than half of the maximal interactions allowed at a given distance, despite the fact that at the pH of 7.5 most of the occupied sites bear full charges. This observation reflects the substantial values of SA assigned to the majority of the charged groups in sperm whale myoglobin (Lee & Richards, 1971; Matthew et al., 1978a; Friend & Gurd, 1979). The maintenance of some considerable degree of solvent exposure for charged groups is probably related to the high solubility of the protein in water. The majority of the strongest stabilizing interactions occur at distances less than 6 or 8 Å, but several substantial ones are seen at greater values of r_{ij}.

Figure 2B is a similar plot dealing with the strongest destabilizing interactions denoted by positive values of $\Delta G_{el}''$. Figure 2B forms a striking contrast with Figure 2A. First, all the destabilizing interactions in Figure 2B are energetically less strong than many of the stabilizing interactions in Figure 2A. Second, much fewer of them fall within the r_{ij} range of 6–8 Å. At the pH of 7.5, potentially destabilizing interactions at the lower r_{ij} values are limited either by particularly high values of SA for both partners or by the failure of a charge to develop on residues such as the histidine residues shown in Figure 2B as filled triangles. The magnitude of the maximally destabilizing interactions is no more than 300 cal/mol at this neutral pH. Constraints are placed on the development of destabilizing interactions by limits on proximity, burial, and charge development between groups of like charge type.

In shifting toward lower pH, there are several predictable changes in the electrostatic interactions among the charged groups. Since the most basic residues, arginine and lysine, are already fully protonated, they sense the changes in electrostatic environments "passively". The strongest stabilizations that the most basic residues enter into involve charge-pair partners whose individual pK values are shifted toward the extremes and so contribute stabilization strongly throughout the pH range from approximately 9 to 3. To discuss the rest of the charge site interactions, on the other hand, it is most informative to present the computed sum of all the interactions

[1] If the distal histidine were given a pK_{int} of 6.00, its computed $pK_{1/2}$ would be close to 5.5, well outside the pH range near 4.5 where it has been found to occur experimentally (Wilbur & Allerhand, 1977; S. H. Friend and F. R. N. Gurd, unpublished experiments). Among several potential reasons for this is its proximity to the electron-withdrawing heme. To approximate these effects, we have arbitrarily set the pK_{int} for His-64 at 5.00 (Botelho et al., 1978). The lower pK_{int} results in a smaller contribution of this residue to the computed destabilizations discussed below.

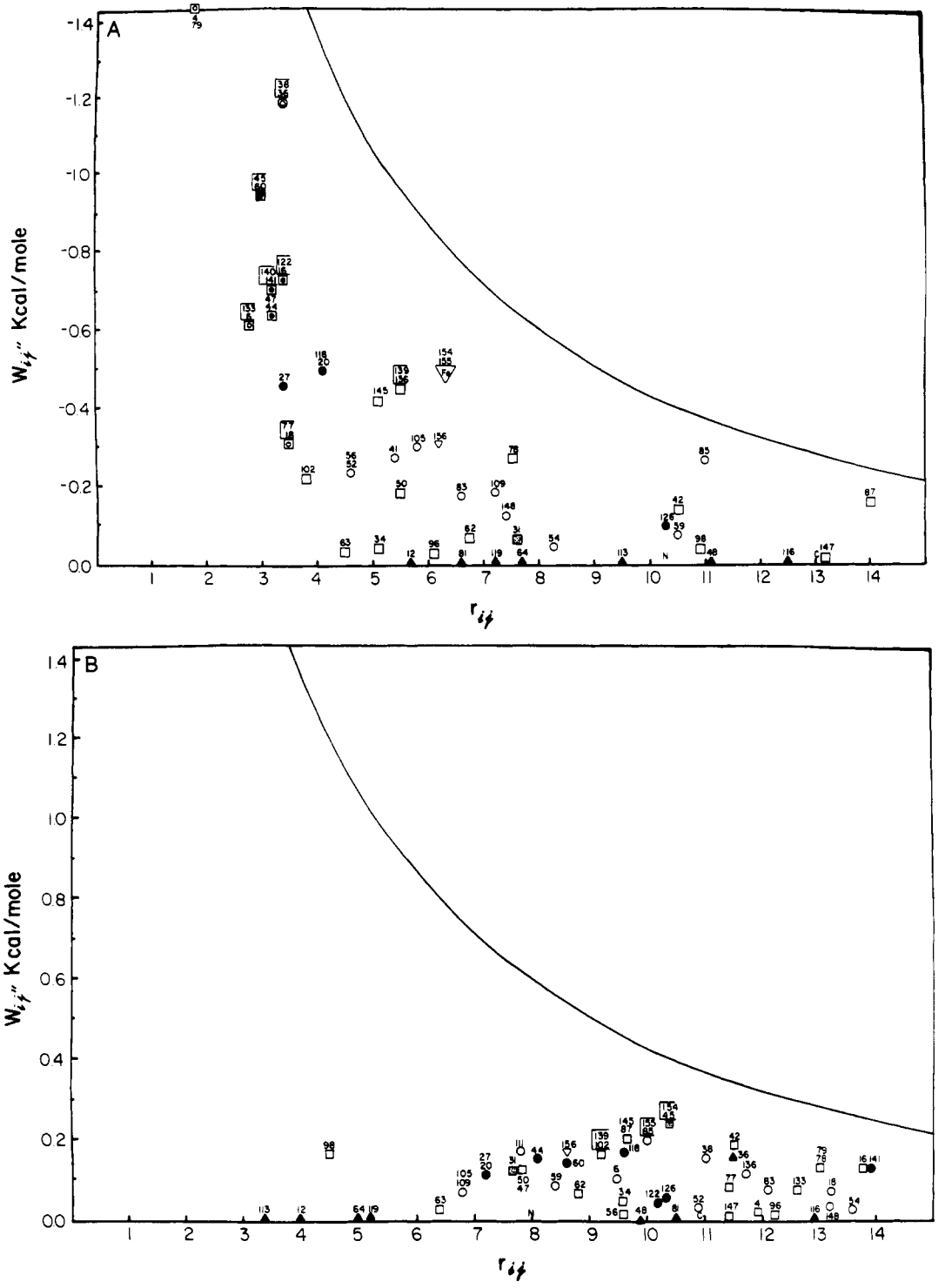

FIGURE 2: (A) Computed maximum stabilizing interaction, W_{ij}'', in kilocalories per mole, experienced by each charged site plotted against the distance in angstroms, r_{ij}, between the numbered site and the oppositely charged site with which that maximum interaction occurs. In the case of the eleven charge pairs, in which the same interaction holds top rank for both members of each pair, both site numbers are shown together. The classes of sites are denoted as follows: (■) Arg; (□) Lys; (Fe) iron atom; (N) NH_2 terminal; (▲) His; (○) Glu; (●) Asp; (C) COOH terminal; (▽) propionic acid. The curve denotes the computed stabilization between fully occupied, oppositely charged sites, each assigned a 1 − SA of 0.95. The conditions are for pH 7.50, an ionic strength of 0.01 M, and 25 °C. (B) The corresponding destabilizing interactions for all charged sites.

between a given residue and all others as a function of pH for each residue.

Electrostatic Environments Sensed by Specific Residues. Parts A and B of Figure 1 have already shown the distribution of stabilizing and destabilizing interactions for the cases of the two sites, Glu-59 and His-64, and Figure 2 has selected the single strongest interactions of each sort for nearly all the groups. We present now in parts A, B, and C of Figure 3 the summed contributions, $\Delta G_{i,el}''$,[2] as a function of pH respectively for each acidic side chain, each titratable histidine residue, and each strongly basic arginine and lysine residue. The computations were made for 25 °C and an ionic strength of

[2] $\Delta G_{i,el}''$ represents the free energy value for the sum of all electrostatic interactions between an ith site and all the jth charged sites, $\sum_{j=1}^{n} W_{ij}''$, achieved, for example, by summing all contributions in Figure 1A.

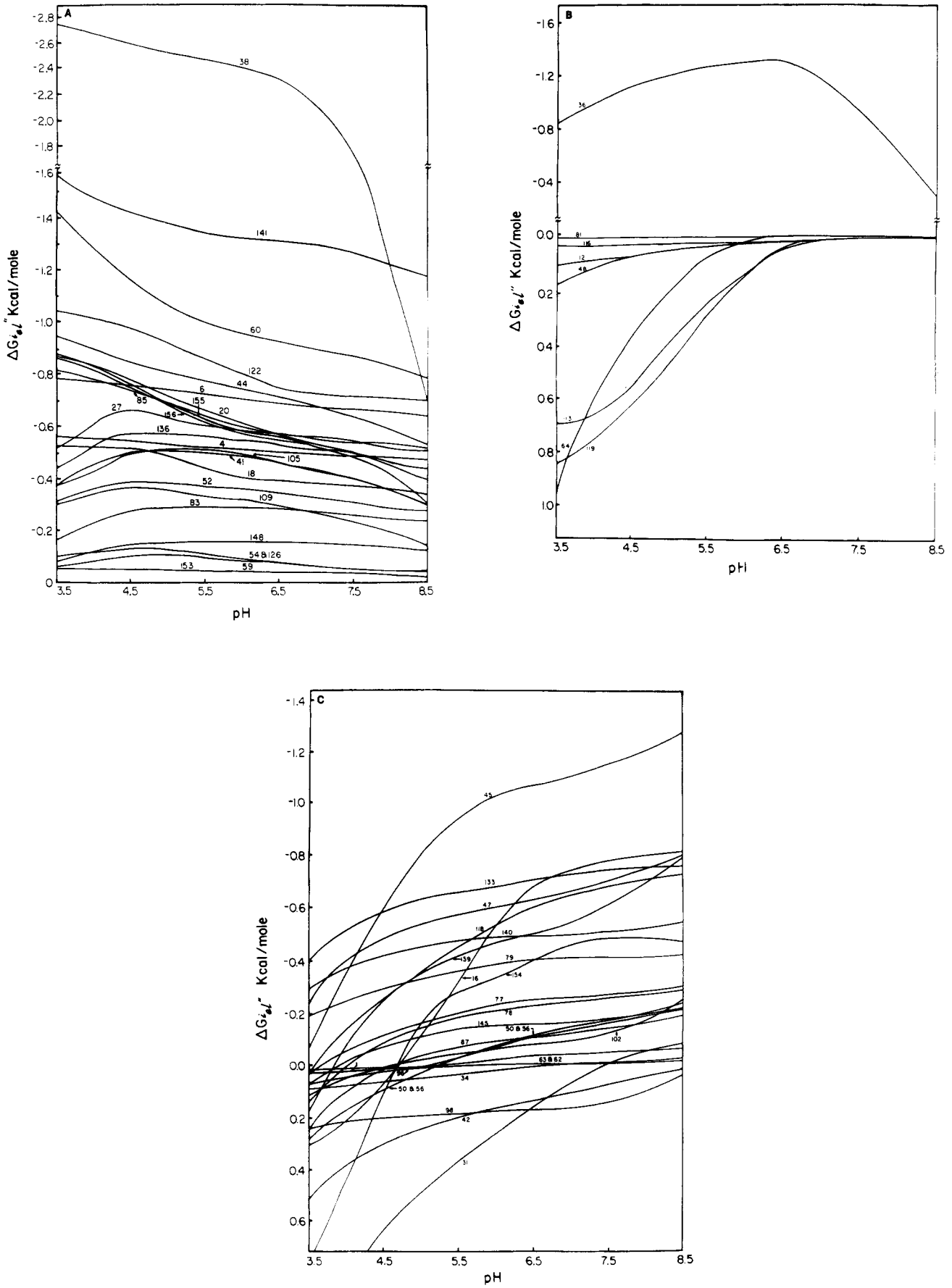

FIGURE 3: (A) Computed free energy contributions, $\Delta G_{i,el}''$, in kilocalories per mole, for acidic groups over the pH range from 3.5 to 8.5. The COOH terminal is denoted by 153. Residues 20, 27, 44, 60, 122, 126, and 141 are aspartic acid. All others are glutamic acid. Note that the scale is condensed beyond −1.6 kcal/mol in the ordinate. The ionic strength is 0.01 M and the temperature is 25 °C. (B) Corresponding plot for histidine residues. Note that the negative ordinate is condensed. (C) Corresponding plot for basic residues. The NH_2 terminal is denoted by 1. Residues 31, 45, 118, and 139 are arginine. The iron atom is denoted by 154. All others are lysine.

0.01 M. The pH range covered is from 3.5 to 8.5, with the isoionic point indicated by an arrow at pH 8.29. In this pH range the tyrosine residues can be omitted from consideration because their anionic form will not occur to a significant extent. At the low end of the pH range the overall sum of all electrostatic free energy remains negative, indicating continued stabilization of the native structure, but the increasing ionic stabilization of the unfolded form containing four additional exposed histidine residues causes the transition to the unfolded form with a midpoint at this ionic strength at pH 3.70 (Friend & Gurd, 1979). We are concerned here only with the native structure.

As shown in Figure 3A, at the isoionic point all the acidic residues sense predominantly stabilizing interactions, that is, effectively a positive environment. The main reason for this stabilization was indicated in Figure 2 by the limitations placed on the interactions between similarly charged groups. Within this generalization there is a 20-fold range in the magnitude of the stabilizations sensed by the individual acidic residues at the isoionic point. The five most stabilizing environments are sensed by groups that are charge paired with oppositely charged groups and that have on the average a 1 − SA value of 0.58. Most of the limitation of SA in these cases derives from the proximity of the paired group. However, overall there is no strong correlation for the acidic residues between the limitation of 1 − SA and the overall value, $\Delta G_{i,el}''$, which means that differences in the distributions of r_{ij} values exert important control.

Figure 3A shows that from pH 8.5 down to pH 5.0 all the acidic residues sense a gradually more positive environment derived from protonation of various histidine residues. Below pH 5.0 some distinctions develop, those acidic residues with higher $pK_{1/2}$ values undergoing some discharge and loss of electrostatic interaction while those with lower $pK_{1/2}$ values continue to sense increasing stabilizations. For example, the effect for Glu-83 with $pK_{1/2}$ of 3.78 contrasts with that for Glu-18 with $pK_{1/2}$ of 2.90. The case of Glu-59, $pK_{1/2}$ of 4.01, represents a near balance between discharge by its own protonation and the change in the electrostatic environment (see Figure 1A and Figure 2). Despite these interactive differences, all acidic residues have as stabilizing, if not more stabilizing, interactions with the rest of the molecule at pH 3.5 as at the isoionic pH, generally follow the same trends, and do not seem to be constrained to any set mode of interactions.

Figure 3B shows the summed interactions in the same terms between each exposed histidine residue and all other charged sites in the molecule. His-36, being taken as involved in a charged pair with Glu-38 (Botelho & Gurd, 1978; Botelho et al., 1978; Friend & Gurd, 1979), takes part in strong net stabilizations over a wide pH range. All the other histidines protonate with relatively low $pK_{1/2}$ values and do not show net interactions above pH 6.75. The four histidine residues with $pK_{1/2}$ values between 5.5 and 6.5, His-48, His-12, His-116, and His-81, sense generally neutral environments and have quite low values of 1 − SA, so that the sums of their interactions produce only mildly destabilizing net effects. The two histidine residues at positions 113 and 119, with $pK_{1/2}$ of 5.35 and 5.42, respectively, well below their pK_{int} values (Friend & Gurd, 1979), sense fairly strong positive environments and so show significantly destabilizing interactions at lower pH in Figure 3B. Their protonation is substantially complete by pH 4.0. The 1 − SA and $pK_{1/2}$ for His-64 are 0.95 and 4.20, respectively, so that this residue senses increasingly severe destabilization below pH 5.5. The primary basis in interactions with the heme iron and Arg-45 has been brought out in Figure 1B. Unlike His-113 and His-119, the destabilization with respect to His-64 continues to be sharply enhanced in the pH range of unfolding (Friend & Gurd, 1979).[1]

Figure 3C shows the pH dependence of the net stabilization or destabilization attributable to electrostatic interactions involving the lysine and arginine residues. As already pointed out, these residues are substantially fully protonated throughout the pH range in question, and so they act passively as probes of the net positive and negative electrostatic environments around them. At the isoionic point, pH 8.29, there is a wide spread of $\Delta G_{i,el}''$, ranging from strongly negative for Arg-45 and Lys-79 to slightly positive for Lys-98 and Lys-42. The proximity of protonating histidine residues is the primary cause of the relative increases in destabilizing interactions that are most notably seen for the curves with the steepest slopes as the pH falls, for instance, those for residues 16, 31, 45, 118, and 139 and the iron atom, 154. The effects of Arg-31 and Arg-45 are the complements of the effects on His-64 (Figure 3B), and the change for Lys-16 is controlled by the primary interaction with His-119 (Figure 3B). As in Figure 3B, a large proportion of the total increase in relative destabilization in the range of acid unfolding can be laid to large changes among a few groups.

The comments relating the separate entries for His-64, His-119, Lys-16, Arg-31, and Arg-45 serve as reminders that the overall summation of all contributions according to $\sum \Delta G_{i,el}''$ will produce double counting. This effect must be allowed for in arriving at an overall summation as described in the preceding paper in this issue (Friend & Gurd, 1979) and applied in Figure 3 therein.

Conservation of the Most Stabilizing Interactions. Bearing in mind the roles of the individual groups in stabilizing and destabilizing interactions, it is natural to enquire whether those that take part in the most strongly stabilizing interactions are preferentially conserved among myoglobins from different animal species in which a considerable number of residue substitutions have been found. Table I lists the various classes of residues in sperm whale myoglobin in order of their decreasing net stabilization in terms of $\Delta G_{i,el}''$ (Figure 3) at pH 7.50, an ionic strength of 0.01 M, and 25 °C. The latter values are shown in a column following the 1 − SA value for the particular residue in question. The next columns list substitutions that have been reported for the residue in question in myoglobins among 53 mammalian species and the frequency of substitution (Friend, 1979). The mammalian myoglobins whose crystal structures have been examined so far fall in either of the two unit cell patterns defined by the sperm whale myoglobin coordinates (Takano, 1977) and the very similar harbor seal myoglobin coordinates (Scouloudi, 1978; Scouloudi & Baker, 1978), so that contacts and restrictions should be apparent from considering variations in the primary structure (Kendrew & Parrish, 1956).

Of the 14 acidic groups involved in stabilizations exceeding 350 cal/mol, 8 represent invariant residues. All the acidic amino acid residues interacting with lesser values for the stabilization energy, furthermore, undergo substitutions; indeed, they are replaced in most instances by an uncharged residue in one or more of the myoglobin species considered.

At the pH of 7.50 considered in Table I, only His-36 shows a strong stabilizing role, $\Delta G_{i,el}''$ being −0.61 kcal/mol. The striking correlation with conservation applies to the residues 36, 64, and 119 that have large values of 1 − SA. Their low values of SA are accentuated for the fully buried residues 24, 82, 93, and 97. Among these residues in mammalian myo-

Table I: Summed Electrostatic Free Energy Contribution of Individual Charge Sites and Their Substitution Frequencies in Myoglobins

residue	1 − SA	$\Delta G_{i,el}''$[a]	substitution[b] residue	frequency
		Acidic Residues		
Glu-38	0.55	−1.73	x	
Asp-141	0.80	−1.31	x	
Asp-60	0.60	−0.88	Glu	2
Asp-122	0.45	−0.75	Glu	8
			Asn	6
			Gln	1
Glu-6	0.50	−0.69	x	
Asp-44	0.60	−0.66	x	
Asp-20	0.50	−0.55	x	
Glu-85	0.75	−0.55	Gln	2
			Asp	1
Asp-27	0.35	−0.55	Glu	36
Glu-136	0.50	−0.52	x	
Glu-4	0.25	−0.49	Asp	49
Glu-105	0.35	−0.43	x	
Glu-41	0.50	−0.42	Ser	2
			Asp	1
Glu-18	0.40	−0.39	x	
Glu-52	0.30	−0.32	Pro	2
			Ala	2
Glu-109	0.30	−0.29	Asp	17
			Gly	1
Glu-83	0.40	−0.29	Asp	8
Glu-148	0.20	−0.14	Val	3
Glu-54	0.25	−0.07	Asp	10
Asp-126	0.30	0.07	Glu	1
Glu-59	0.30	−0.05	Ala	2
Prop-155	0.70	−0.52	x	
Prop-156	0.50	−0.26	x	
Gly-153	0.10	−0.04	x	
		Histidine Residues		
His-36	0.85	−0.61	x	
His-64	0.95	0.00	x	
His-81	0.05	0.00	Gln	8
His-12	0.15	0.00	Asn	45
His-116	0.05	+0.01	Gln	21
His-48	0.30	+0.02	Asn	2
His-113	0.35	+0.06	Gln	15
His-119	0.80	+0.06	x	
		Basic Residues		
Arg-45	0.75	−1.14	Lys	54
Lys-16	0.90	−0.75	x	
Lys-133	0.60	−0.70	x	
Lys-47	0.55	−0.69	x	
Arg-118	0.70	−0.66	Lys	41
Arg-139	0.95	−0.59	x	
Lys-140	0.45	−0.49	Asn	33
Lys-79	0.45	−0.42	x	
Lys-77	0.45	−0.24	x	
Lys-78	0.60	−0.22	x	
Lys-145	0.50	−0.16	Asn	6
			Gln	3
			Glu	1
Lys-56	0.65	−0.15	Arg	3
Lys-50	0.40	−0.13	x	
Lys-87	0.95	−0.10	Ala	1
Lys-102	0.40	−0.10	Gln	1
Lys-63	0.05	−0.08	x	
Lys-62	0.20	−0.08	Arg	2
Lys-96	0.05	−0.02	x	
Lys-34	0.15	−0.01	Thr	10
Arg-31	0.40	+0.05	Ser	1
Lys-42	0.75	+0.09	x	
Lys-98	0.20	+0.17	x	
Fe-154	0.95	−0.45	x	
Val-1	0.05	−0.01	Gly	49

[a] pH 7.50, an ionic strength of 0.01 M, and 25 °C. [b] Substitutions among 53 mammalian myoglobins (Friend, 1979); x denotes invariant residue.

Table II: Electrostatic Stabilization through Charge Pairs

paired residues	W_{ij}'' (kcal/mol)	r_{ij} (Å)	pairing by region	charge-pair retention index
Glu-4, Lys-79	−1.44[a]	1.8	A-EF[b]	100[c]
Glu-38, His-36	−1.20	3.4	C-C	100
Asp-60, Lys-45	−0.96	3.0	E-CD	100
Asp-122, Lys-16	−0.74	3.4	GH-A	88
Asp-141, Lys-140	−0.71	3.3	H-H	42
Asp-44, Lys-47	−0.65	3.2	CD-CD	100
Glu-6, Lys-133	−0.62	2.8	A-H	100
Asp-20, Arg-118	−0.50	4.1	B-G	100
Prop-155, Fe-154	−0.48	3.5	heme-heme	100
Glu-136, Arg-139	−0.46	5.5	H-H	100
Glu-18, Lys-77	−0.32	3.5	A-EF	100
Glu-52, Lys-56	−0.24	4.6	D-D	93

[a] pH 7.50, an ionic strength of 0.01 M, and 25 °C. [b] In accordance with the standard nomenclature (Watson, 1969), a single letter refers to a given helical segment, whereas two letters are used to denote an interhelical segment between the corresponding two helices. [c] Percentage retention of both charge types among 53 varieties of mammalian myoglobin.

globins only His-82 has been reported substituted for glutamine in one species, the badger (Tetraert et al., 1974). For the histidine residues, therefore, low values of SA between 0.00 and 0.20 correlate best with conservation. This is not to say that in related groups of animals conservation of certain of the more exposed histidine residues and of their individual electrostatic environments is not the rule (Botelho & Gurd, 1978). Presumably, such conservation is related in some way to function rather than necessarily or exclusively to stability as such. An example of such a functional adaptation would be the provision of buffering power in the functional pH range of the muscle cell (Matthew et al., 1979a).

Turning finally to the lysine and arginine class of charged groups, we find that a heirarchical order as seen for the acidic residues in Table I is again illustrated. Nine of the ten residues that contribute more than 200 cal/mol of net stabilization through their electrostatic interactions are conserved as positively charged forms, whereas among the twelve groups falling farther down the scale eight are conserved as positively charged forms among the various mammalian myoglobin species.

Returning to the consideration of pairwise interactions, Table II lists the individual W_{ij}'' values in kilocalories per mole between charge-pair partners at pH 7.50, an ionic strength of 0.01 M, and 25 °C. All the sites involved bear full formal charges under these conditions, so that W_{ij}'' corresponds to $\Delta G_{el}''$. Table II lists in addition the separation between the paired sites and the regions of the molecule involved in the specified stabilizing interactions. The last column denotes a charge-pair retention index showing the percentage retention of charge at both charge sites among the 53 species of mammalian myoglobin considered. This index counts as retained a pair in which the acidic residue is replaced by another acidic residue or the basic by another basic residue without the loss of the pairwise electrostatic interaction. Note that the retention index is most often 100, with only the one much lower value for Asp-141 with Lys-140 of 42. In that case the interaction of adjacent residues in the H helix may be reinforced by the interaction of Glu-136 with Arg-139 on the other side of the helix.

Clearly, the charge pairs listed in Table II are essential structural features of the myoglobin molecule. The W_{ij}'' values listed here sum to −7.8 kcal/mol (omitting the heme entry) out of a net sum for all interactions under these conditions of

approximately −9.7 kcal/mol (Friend & Gurd, 1979). These charge-pair interactions determine the scale of the stabilizing interactions without reflecting the pH dependence of the net free energy values over the range between pH 8.5 and 3.5.

Changes in Local Electrostatic Environments with pH. The pH dependence of the stabilizing and destabilizing interactions between specific residues can also be usefully visualized in terms of computed potential energy maps covering various segments of the molecular surface. Such maps were generated to show the changes in stabilization sensed at individual sites as the pH was lowered from 6.5 to 3.5 under conditions of 25 °C and an ionic strength of 0.01 M. The potential energy maps were created by first projecting the coordinates of charged groups onto an imaginary shell with a radius of 18 Å passing through the center of the molecule. This shell was then unfolded into six sections by projecting the structure onto the two-dimensional surfaces of a cube. Distortions caused by variations in the distance to the shell were less than 5 Å, and the problem of distortion at the edges of the 20-Å scans was largely overcome by the location of most charged groups on several of these projections. To allow for the changes in $\Delta G_{i,el}''$ for a given site in passing from pH 6.5 to pH 3.5, we represent the resulting net destabilization or stabilization by a hill or a valley in which each grid width in height represents 150 cal/mol. The change in interaction energy with the pH change is of greater interest at this stage than the absolute magnitude; it will be recalled that in the native structure the total net electrostatic free energy retains a substantial negative value even at pH 3.5.

Figure 4A shows a scan around Lys-77 to show the adjacent difference surface defined above in passing from pH 6.5 to 3.5. The planar grid indicates approximately the geometrical spacing of the charged sites, whereas the elevations or depressions indicate the effect of the pH change on the electrostatic summations reflecting, in addition, the influence of the 1 − SA terms in eq 1. Two major areas of interest in this projection are in the lower right and upper left corners. The first depicts the changes sensed in the A helix by His-12 and Lys-16 and in the GH corner by His-119 and Asp-122. The Lys-16 site is 4.0 Å from that on His-12, $pK_{1/2}$ of 5.7, and 4.1 Å from that on His-119, $pK_{1/2}$ of 5.4. The His-119 residue, nevertheless, senses a much greater destabilization because its 1 − SA value is 0.80, whereas that of His-12 is only 0.10 (see also Figure 3B). Asp-122 with its $pK_{1/2}$ of 2.30 remains fully charged and senses a slight stabilizing effect of the nearby protonations indicated by the small declivity. This region of the map emphasizes, therefore, a primary destabilizing interaction between Lys-16 and the newly charged His-119 residue, each on a separate structural segment of the protein.

The second area of major interest, in the upper left part of Figure 4A, depicts the changes sensed in the E- and F-helix regions involving mainly Lys-77, Lys-78, Glu-83, Glu-85, and Lys-87. The most important parts of this cluster are the positive Lys-78 and Lys-87 which are not far from Glu-83 and Glu-85; the latter have $pK_{1/2}$ values of 3.68 and 3.78, respectively. Note that as these acid residues begin to protonate the Lys-78 and Lys-87 sense net destabilizations. The protonation of Glu-83 and Glu-85, however, lessens their mutual destabilization, thereby minimizing the elevations at these points.

Figure 4B is a scan around Glu-41 that illustrates the changes computed in the region of the heme pocket as the pH is lowered from 6.5 to 3.5. Included are the charge pair, above, of the His-36 with Glu-38 in the C helix, another pair, in the lower right, Asp-60 with Arg-45, the His-64 and Fe-154 along

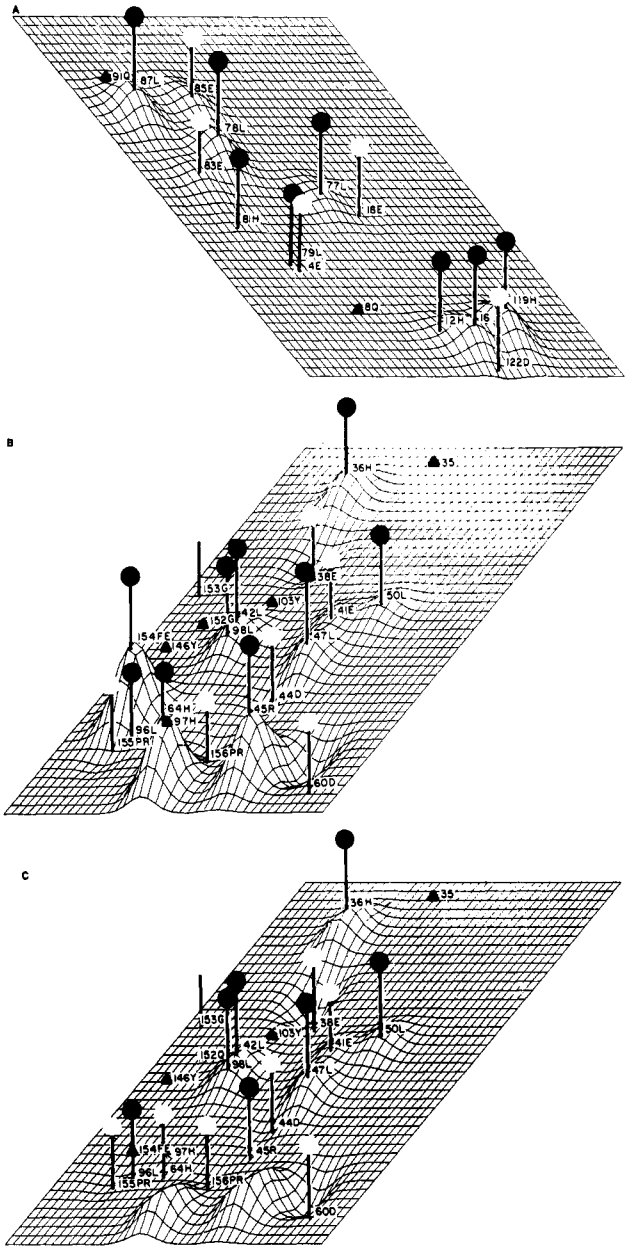

FIGURE 4: (A) Potential energy difference surface depicting the change in $\Delta G_{i,el}''$ for various sites around Lys-77 in ferrimyoglobin in passing from pH 6.5 to pH 3.5. Each grid width in height represents 150 cal/mol. The individual sites are identified by residue number and amino acid type in the one-letter code. Positive groups are shown in black; negative groups are shown in white. The fractional site occupancy at the midpoint of the acid unfolding, pH 3.70, is indicated by the height of the pole. Solid triangles indicate site occupancy of less than 0.1. The computations are made for an ionic strength of 0.01 M and 25 °C. (B) Corresponding plot around Glu-41. (C) Plot corresponding to (B) except that the electrostatic interactions are modified by azide ligation to discharge the iron site. The points denoting uncharged site locations are included for future comparison with myoglobins of other species (Botelho et al., 1978).

with the propionic acid groups 155 and 156, and several less prominent features. His-36, Lys-42, Lys-47, and Lys-50 are all destabilized by the increasingly positive charge on this portion of the molecule produced, for example, by the protonation of Glu-41 with its $pK_{1/2}$ of 3.56. This particular protonation produces in turn small stabilizing changes at considerable distances, e.g., of Glu-38 at 12.2 Å, Glu-105 at 11.1 Å, and Glu-109 at 13.3 Å.

In the lower part of Figure 4B are shown the three most important destabilizing changes in the molecule sensed by

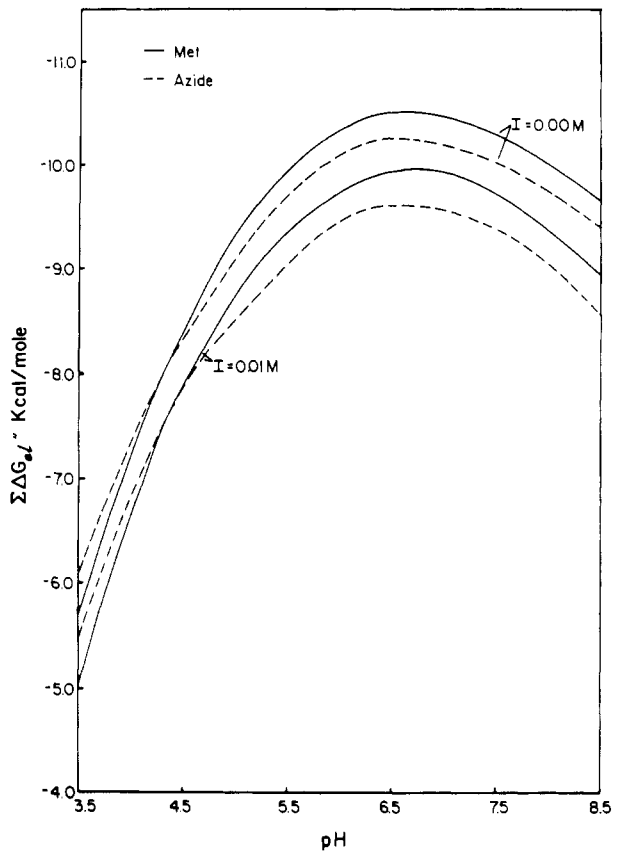

FIGURE 5: Plot of summed free energy contribution from all charge site interactions as a function of pH for both the azide (---) and ferri (—) forms for the ionic strengths 0.00 and 0.1 M [see Figure 3 of Friend & Gurd (1979)].

Fe-154, His-64, and Arg-45. The protonation of His-64, 1 - SA of 0.95, lying only 5.0 Å from Arg-45 and 5.8 Å from the iron atom, is responsible for a change of over 500 cal/mol sensed by each of these groups. In contrast, Asp-60 and the propionic acid groups 155 and 156 are slightly stabilized by this protonation event. Note that the three dominant groups, His-64, Arg-45, and the iron atom, are representative of three separate structural segments of the holoprotein, the E helix, the CD segment, and the heme, respectively.

Effect of Neutralizing the Iron Charge with Azide Ion. The most striking feature of Figure 4B is the set of mutual destabilizations experienced by the three positive sites in the heme-pocket region just discussed. The positive charge assigned to the iron atom in the ferrimyoglobin can be neutralized in theory and in practice by the binding of azide ion. Stryer et al. (1964) established that the binding of azide in the crystalline state produced only very slight structural alterations. It is known that full occupancy of the iron site by the azide can be achieved even in the pH range down to 3.5 (Nakhleh, 1971). Figure 4C shows the computed scan around Glu-41, exactly comparable to Figure 4B, when the iron atom is taken to be discharged by combination with the azide ion. In contrast with Figure 4B, Figure 4C shows the absence of a change with pH in the stabilization sensed by His-64, as well as the absence of a change at the neutralized iron atom as the pH is lowered from 6.5 to 3.5. Other parts of the region reflect few changes.

Figure 5 shows the summed curves for $\sum\Delta G_{el}''$ covering all charged sites in the protein as a function of pH, according to the treatment in Figure 3 of the preceding paper in this issue (Friend & Gurd, 1979), in the presence and absence of azide bound to the iron atom. In each case the computations are

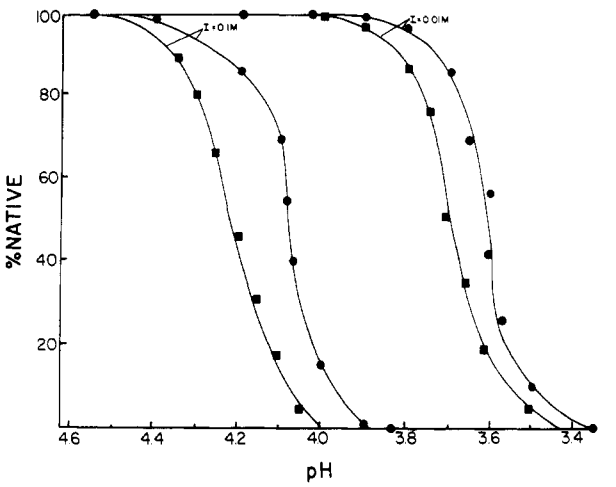

FIGURE 6: Dependence of unfolding transition of sperm whale ferrimyoglobin (■) and azide myoglobin (●) on pH plotted as percent remaining native form for ionic strengths 0.01 and 0.10 M. Results monitored by absorbance at 409 nm or by circular dichroism at 222 nm were overlaid.

shown for zero ionic strength and for 0.01 M. The curves show that at pH values above the protonation range of His-64 the electrostatic consequences of binding of azide are to lower the net stabilization by a small amount, reflecting the destabilization of anionic sites mentioned above. Below pH 4.5 the effect of the azide binding is to promote net stabilization by a little over 300 cal/mol. At an ionic strength of 0.10 M this difference in stability in the presence of azide would shift the midpoint of the acid unfolding downward by approximately 0.1 pH unit (Friend & Gurd, 1979).

To test this prediction experimentally, we tested the effect of azide on the unfolding profiles in acid solution (Friend & Gurd, 1979) for ionic strength values of 0.01 and 0.10 M, as shown in Figure 6. At both ionic strength values the azide derivative is indeed the more stable whether monitored by absorbance of the Soret band or ellipticity at 222 nm. The curves in the presence of azide appear somewhat steeper than those in its absence although the dependence on ionic strength is nearly equivalent and establishes the basis of the transition in ionic processes (Friend & Gurd, 1979). The presence of the heme is responsible for a far more cooperative transition in the holoprotein than in the apoprotein (Breslow et al., 1965). The effect may be enhanced in the present instance by the coupled equilibrium with the excess azide. While the replacement of water with azide as the sixth heme ligand would be expected to strengthen the bond between the iron and His-93 (Breslow et al., 1965; McLendon & Sandberg, 1978), the extent of stabilization of the acid-denatured state by azide may well be comparable. Azide ion binding has been shown to have some stabilizing effect at neutral pH in concentrated guanidinium hydrochloride solution (McLendon & Sandberg, 1978).

The results presented above provide some answers to the questions posed in the introduction. First, numerous examples have been given of changes in the pattern of stabilizing or destabilizing electrostatic interactions experienced by a given group when one or more neighboring groups undergo titration. Second, it is possible to draw from the data developed here sums of stabilizing and destabilizing electrostatic interactions under given conditions. For the net stabilizing free energy at pH 6.5, an ionic strength of 0.01 M, and 25 °C of −9.90 kcal/mol (Friend & Gurd, 1979), the sum of the negative $\Delta G_{el}''$ terms is −10.25 kcal/mol and the sum of the positive $\Delta G_{el}''$ terms is +0.35 kcal/mol. The corresponding three

values at pH 4.0 are −5.02, −8.72, and +3.70 kcal/mol, respectively. Third, it is evident that the electrostatic interaction patterns of individual sites of a given amino acid type do indeed vary widely. Fourth, clear evidence has been given of preferential conservation during evolution of those individual charge-bearing residues that take part in the most highly stabilizing electrostatic interactions. Fifth, as is shown best in Figure 4B, destabilizing interactions can indeed accumulate in a given region of the structure in connection with the unfolding process in acid solution. These destabilizing interactions offset in part the relatively pH-independent, stabilizing charge-pair interactions. Since the electrostatic interactions necessarily involve pairs of charged sites, neutralizing one site may obviate much of the effect of a destabilizing cluster (Figure 4C).

Minor Role of a "Trigger Group". It is common practice to identify an ionizing group such as His-64 with a "trigger" role if, as observed here, its $pK_{1/2}$ corresponds to the midpoint pH of a conformational transition (Tanford, 1970; Puett, 1973). From Figure 3, it may be seen that the slope at the midpoint of the change in $\Delta G_{el}''$ with pH, $\partial \Delta G_{el}''/\partial$pH, is indeed steep for His-64. However, it can be estimated from the individual curves that His-64 contributes only 11% of the net slope; Arg-31 and Lys-42 also show especially rapid changes, for example. The overall transition will combine $\partial \Delta G_{el}/\partial$ pH terms for both the native and the denatured forms to produce the narrow, cooperative transition profile (Figure 6), thereby lowering the fractional contribution attributable to His-64 by a further factor of comparable or greater magnitude. Conversely, the analysis of the relation between titration of certain individual residues and any pH-dependent conformational changes outside of the unfolding region may prove especially fruitful (S. H. Friend, T. M. Rothgeb, R. S. Gurd, H. Scouloudi, and F. R. N. Gurd, unpublished experiments).

Nucleation and Docking in Chain Folding. The contribution of the virtual charges associated with the α-helix dipoles (Hol et al., 1978; Friend & Gurd, 1979) may be of greatest relevance to the formal Coulombic interactions dealt with here when the role of charge interactions in nucleation and folding is considered (Richmond & Richards, 1978). Table II has introduced the observation that the computed electrostatic interaction energy, $\Delta G_{el}''$, experienced by individual pairs of sites is most stabilizing when certain such sites are charge paired and that such charge pairing appears to be conserved in evolution. The listing in Table II also draws attention to those charge pairs that achieve stabilization within a given helix and those that stabilize the relationships between different helix segments. Both modes are well represented. The strong pairs Glu-38 with His-36 and Asp-141 with Lys-140 are intrahelical and can be expected to promote the nucleation of the C and H helices, respectively. The strong pairs Glu-4 with Lys-79, Asp-60 with Arg-45, Asp-122 with Lys-16, and Glu-6 with Lys-133 can be expected to promote orientation and docking of the following structural regions respectively: A helix with E helix; E helix with CD corner; GH corner with A helix; A helix with H helix. Table II lists, in addition, two weaker intrahelical pairs, Glu-136 with Arg-139 in the H helix and Glu-52 with Lys-56 in the D helix. These illustrations serve to point up four examples of intrahelical nucleation potentiality affecting the C, D, and H helices and also four examples of nucleation potentiality between regions that promote apposition of the A helix with the E and H helices and with the GH corner, as well as of the E helix with the CD corner (Ptitsyn et al., 1972; Ptitsyn & Raskin, 1973; Anfinsen & Scheraga, 1975; Richmond & Richards, 1978). In the holoprotein the electrostatic interactions of the propionic acid groups of the heme serve to anchor the prosthetic moiety to the FG region and can be considered in conjunction with the coordinate bond between the iron atom and His-93.

The role in nucleation of the virtual charges associated with the α-helix dipoles can be considered in the same two contexts, the nucleation of helices and the orientation and docking of the structural regions. Reference to Table I of the preceding paper in this issue (Friend & Gurd, 1979) shows several examples, such as Glu-4, Lys-34, and Lys-78, in which a residue of charge type opposite to the appropriate dipole virtual charge is present on or very near the helix terminus in question. The argument is readily extended to draw on stabilization between structural regions. Very probably, the relative importance of the dipole virtual charges will be greatest at the initial nucleation stages in controlling the length of helical segments and in the initial condensation and docking stages where the average separation of the formal charge sites will be generally greater so that their net stabilizing influence is not yet fully developed. In this context a similar role may be played by the conserved internal histidine residues 24 and 82 that may contribute transiently in the charged state to the control of the formation of the corners involving respectively the A, B, and C helices and the A, E, and F helices.

Richmond & Richards (1978) examined the geometry of docking of helices in myoglobin. They found, for example, that, if the A helix was considered to be separated out into the solvent from the rest of the structure along a normal to its axis and was allowed to return to its observed position in the structure, then the displacement of intervening solvent molecules became accentuated as the separation distance was reduced to 6 Å. The computations in Figure 2 illustrate the potentialities for Coulombic interactions at separations of 6–8 Å or more, before the important packing interactions can become fully developed (Gurd & Rothgeb, 1979). While the results of the present treatment of interactions between charges in a spherical geometry cannot be applied quantitatively before the last stages of condensation of the polypeptide chain into the compact native structure, they can serve as a useful qualitative guide.

Acknowledgments

The advice and encouragement of Professor G. I. H. Hanania, Dr. J. B. Matthew, and Dr. T. M. Rothgeb are gratefully acknowledged. Professor J. Hepner gave invaluable help in the construction of computer graphics.

References

Acampora, G., & Hermans, J., Jr. (1967) *J. Am. Chem. Soc. 89*, 1543.

Anfinsen, C. B., & Scheraga, H. A. (1975) *Adv. Protein Chem. 29*, 206.

Botelho, L. H., & Gurd, F. R. N. (1978) *Biochemistry 17*, 5188.

Botelho, L. H., Friend, S. H., Matthew, J. B., Lehman, L. D., Hanania, G. I. H., & Gurd, F. R. N. (1978) *Biochemistry 17*, 5197.

Breslow, E., Beychok, S., Hardman, K. D., & Gurd, F. R. N. (1965) *J. Biol. Chem. 240*, 304.

Clark, J. F., & Gurd, F. R. N. (1967) *J. Biol. Chem. 242*, 3257.

Friend, S. H. (1979) Ph.D. Thesis, Indiana University, Bloomington, IN.

Friend, S. H., & Gurd, F. R. N. (1979) *Biochemistry* (preceding paper in this issue).

Gurd, F. R. N., & Rothgeb, T. M. (1979) *Adv. Protein Chem.* (in press).
Hol, W. G. J., van Duijnen, P. T., & Berendsen, H. J. C. (1978) *Nature (London) 273*, 443.
Kendrew, J. C., & Parrish, R. G. (1956) *Proc. R. Soc. London, Ser. A 238*, 305.
Lee, B., & Richards, F. M. (1971) *J. Mol. Biol. 55*, 379.
Linderstrøm-Lang, K. (1924) *C. R. Trav. Lab. Carlsberg 15*, 70.
Matthew, J. B., Hanania, G. I. H., & Gurd, F. R. N. (1978a) *Biochem. Biophys. Res. Commun. 81*, 410.
Matthew, J. B., Friend, S. H., Botelho, L. H., Lehman, L. D., Hanania, G. I. H., & Gurd, F. R. N. (1978b) *Biochem. Biophys. Res. Commun. 81*, 416.
Matthew, J. B., Hanania, G. I. H., & Gurd, F. R. N. (1979a) *Biochemistry 18*, 1919.
Matthew, J. B., Hanania, G. I. H., & Gurd, F. R. N. (1979b) *Biochemistry 18*, 1928.
McLendon, G., & Sandberg, K. (1978) *J. Biol. Chem. 253*, 3913.
Nakhleh, E. (1971) Ph.D. Thesis, American University of Beirut.
Ptitsyn, O. B., & Raskin, A. A. (1973) *Dokl. Akad. Nauk SSSR 213*, 473.
Ptitsyn, O. B., Lim, V. I., & Finkelstein, A. V. (1972) *FEBS Lett. 25*, 421.
Puett, D. (1973) *J. Biol. Chem. 248*, 4623.
Richmond, T. J., & Richards, F. M. (1978) *J. Mol. Biol. 119*, 537.
Scouloudi, H. (1978) *J. Mol. Biol. 126*, 661.
Scouloudi, H., & Baker, E. H. (1978) *J. Mol. Biol. 126*, 637.
Shire, S. J., Hanania, G. I. H., & Gurd, F. R. N. (1974a) *Biochemistry 13*, 2967.
Shire, S. J., Hanania, G. I. H., & Gurd, F. R. N. (1974b) *Biochemistry 13*, 2974.
Shire, S. J., Hanania, G. I. H., & Gurd, F. R. N. (1975) *Biochemistry 14*, 1352.
Stryer, L., Kendrew, J. C., & Watson, H. C. (1964) *J. Mol. Biol. 8*, 96.
Takano, T. (1977) *J. Mol. Biol. 110*, 537.
Tanford, C. (1961) *Physical Chemistry of Macromolecules*, p 571, Wiley, New York.
Tanford, C. (1970) *Adv. Protein Chem. 24*, 1.
Tanford, C., & Kirkwood, J. G. (1957) *J. Am. Chem. Soc. 79*, 5333.
Tanford, C., & Roxby, R. (1972) *Biochemistry 11*, 2192.
Tetaert, D., Han, K. K., Plancot, M. T., Dautrevaux, M., Ducastiang, S., Hombrados, I., & Neuzil, E. (1974) *Biochim. Biophys. Acta 351*, 317.
Watson, H. C. (1969) *Prog. Stereochem. 4*, 299.
Wilbur, D. J., & Allerhand, A. (1977) *J. Biol. Chem. 252*, 4968.

Stereochemistry of the Hydrolysis of the Endo Isomer of Uridine 2′,3′-Cyclic Phosphorothioate Catalyzed by the Nonspecific Phosphohydrolase from *Enterobacter aerogenes*†

John A. Gerlt* and Winnie H. Y. Wan

ABSTRACT: The nonspecific phosphohydrolase from *Enterobacter aerogenes* (ATCC 13048) requires divalent metal ions for activity, since zinc present in the isolated enzyme can be removed by extensive dialysis against 8-hydroxyquinoline-5-sulfonate at pH 7.5 to yield an inactive enzyme which can be reactivated by addition of Zn^{2+}, Cd^{2+}, Co^{2+}, Mn^{2+}, or Ni^{2+}; six ions of either zinc or cadmium can be incorporated into the inactive enzyme, and this incorporation of metal ion can be correlated with the regaining of activity (J. A. Gerlt, R. Dhesi, and H. C. Hemmings, unpublished experiments). The cadmium-reactivated phosphohydrolase catalyzes the hydrolysis of the endo isomer of uridine 2′,3′-cyclic phosphorothioate (U>pS) to yield uridine 3′-monophosphorothioate as the major product. After enzymatic hydrolysis of the cyclic phosphorothioate in 19.8% $H_2{}^{18}O$ and chemical recyclization of the ^{18}O-labeled acyclic phosphorothioates to yield a mixture of the endo and exo isomers of U>pS, ^{18}O is found primarily in the exo isomer, as judged by examination of the 145.7-MHz phosphorus-31 nuclear magnetic resonance spectrum of the mixture. This observation indicates that the cadmium phosphohydrolase catalyzes hydrolysis of *endo*-U>pS with inversion of configuration, implying that the hydrolysis reaction proceeds by an in-line attack of water on the phosphorus.

Enzymes which catalyze the hydrolysis of phosphodiester bonds are ubiquitous in nature and are crucial to many biochemical processes. For example, cAMP[1] phosphodiesterase catalyzes the hydrolysis of the 3′-ester bond in cAMP, providing the only known pathway by which this important regulatory nucleotide can be inactivated and returned to the acyclic adenine nucleotide pool. Nucleases are involved in a wide variety of in vivo and in vitro processes, including repair of genetic damage induced by mutagens and the construction of recombinant DNA molecules which are useful in gene

† From the Department of Chemistry, Yale University, New Haven, Connecticut 06520. *Received May 7, 1979.* This work was supported by the National Institutes of Health, Grant GM-22350. J.A.G. is a Research Career Development Awardee of the National Cancer Institute (CA 00499).

[1] Abbreviations used: cAMP, adenosine 3′,5′-cyclic monophosphate; NMR, nuclear magnetic resonance; EDTA, ethylenediamine-*N*,*N*′-tetraacetic acid; Mops, morpholine-*N*-(3-propanesulfonic acid); Ches, cyclohexylamine-*N*-(2-ethanesulfonic acid); HQSA, 8-hydroxyquinoline-5-sulfonic acid; U>p, uridine 2′,3′-cyclic monophosphate; U>pS, uridine 2′,3′-cyclic phosphorothioate; UMP, uridine monophosphate; UMPS, uridine monophosphorothioate; TLC, thin-layer chromatography; ATPαS, adenosine 5′-*O*-(1-thiotriphosphate); ATPβS, adenosine 5′-*O*-(2-thiotriphosphate); $NaDodSO_4$, sodium dodecyl sulfate; DEAE, diethylaminoethyl.

0006-2960/79/0418-4630$01.00/0